Available online at www.sciencedirect.com
SCIENCE DIRECT
Trans. Nonferrous Met. Soc. China 16(2006) 1064−1068
Transactions of Nonferrous Metals Society of China
www.csu.edu.cn/ysxb/

Atom exchange of martensite in Cu-13Zn-15Al alloy during non-isothermal aging

LI Zhou(李 周)[1,2], XIAO Zhu(肖 柱)[1,2], BAO Ji-qing(保吉庆)[3], XU Gen-ying(徐根应)[1,2], ZHENG Feng(郑 峰)[1,2]

1. School of Materials Science and Engineering, Central South University, Changsha 410083, China;
2. Key Laboratory of Nonferrous Metal Materials Science and Engineering, Ministry of Education, Central South University, Changsha 410083, China;
3. College of Biology and Chemical Engineering, Jiaxing University, Jiaxing 314001, China

Received 2 December 2005; accepted 20 April 2006

Abstract: The bulk specimens with preferable orientation were utilized to investigate atom exchange of martensite in Cu-13Zn-15Al alloy during non-isothermal aging by in-situ X-ray diffraction. It is found that the exchange of Zn atoms at position Ⅲ and Cu atoms at Ⅱ and the exchange of Zn atoms at position Ⅲ and Al atoms at Ⅰ on the basal plane of martensite occur during heating at a heating rate of 5 ℃/min. 13% (2/25) of Al atoms transfer from position Ⅰ to position Ⅲ when temperature goes up to 160 ℃.

Key words: Cu-Zn-Al shape memory alloy; martensite; atom exchange

1 Introduction

Cu-Zn-Al alloys as well as Ni-Ti alloys are known to exhibit the shape memory effect, being associated with a thermoelastic martensite transformation and its reversion[1−4]. Cu-Zn-Al alloys are less stable than the Ni-Ti alloys above room temperature. In fact, the reverse transformation start and finish temperatures (A_s and A_f) increase during keeping in the martensite phase[5−7]. This phenomenon, which is often called "the stabilization of martensite", is a serious problem in the application of this alloy in practical use above room temperature. Many researches have been conducted to study the stabilization of martensite, and some mechanism has been uncovered[8−14]. NAKATA et al[6] reported that the exchange of Zn atoms in β-plane and Cu atoms in α-plane takes place during aging with ALCHEMI method[15]. The above analysis of ALCHEMI measurements is based on the assumption that Al atoms do not change their positions. However, this is not the case. In the present paper, the bulk specimen of preferable orientation is utilized to investigate Al atoms' rearrangement in the martensite of Cu-13Zn-15Al alloy during non-isothermal aging by in-situ X-ray diffraction.

2 Experimental

The tested alloy Cu-13Zn-15Al (mole fraction, %) was prepared by induction melting and homogenized at 850 ℃ for 24 h, and finally rolled to 1 mm thickness plate. The plate was then cut into small pieces for subsequent examinations. The specimens were solid-solution treated at 850 ℃ for 10 min and then quenched into water. The transformation temperature A_s was measured by electrical resistance method. A_s of 190 ℃ at the heating rate of 25 ℃/min and 320 ℃ at the heating rate of 5 ℃/min have been obtained. The martensite stabilization occurred as the heating rate was 5 ℃/min. X-ray diffraction examination was made in a D-Max2500 diffractometer with Cu K_α radiation with powder specimen and bulk specimen. The powder specimen, which had passed through a 300-mesh sieve (<46 μm) and had been solution-treated at 850 ℃ for 10 min in an evacuated quartz capsule then water-quenched, was utilized to determine the crystal parameters. The bulk specimen with preferable orienta-

Foundation item: Project(05JJ3005) supported by the Natural Science Foundation of Hunan Province, China; Project(20040553069) supported by the PhD Programs of Ministry of Education of China
Corresponding author: LI Zhou; Tel: +86-731-8830264; Fax: +86-731-8876692; E-mail: lizhou6931@163.com

orientation treated with the same method was utilized to measure the variation of the superstructure diffraction during heating because the intensity of the superstructure diffraction peak in the martensite of the tested alloy measured by powder specimen was too weak to be sensitively checked. The relative variation amount of integrated intensity of a specific diffraction peak obtained with the bulk specimen during successive heating is the same as that with the powder specimen by in-situ X-ray diffraction measurement.

3 Experimental results

Fig.1 shows the X-ray diffraction spectra of the tested alloy during heating at a heating rate of 5 ℃/min. Information about the structure can be acquired as follows: 1) The structure of the martensite as-quenched in the alloy is M18R (see Fig.1(a))[16]; 2) within 160 ℃, the $(12l)_M$ and $(20\bar{l})_M$, $(04\bar{l})_M$ and $(34\bar{l})_M$ diffraction pairs tend to get closer during heating, the monoclinic angle β tends to 90° and most of them merge into one diffraction peak at 160 ℃, respectively. That is, the structure transforms from M18R (monoclinic 18R) into N18R (normal 18R) according to the formula as follows:

$$\frac{1}{d^2}=\frac{h^2}{a^2\sin^2\beta}+\frac{k^2}{b^2}+\frac{l^2}{c^2\sin^2\beta}-\frac{2hl\cos\beta}{ac\sin^2\beta} \quad (1)$$

The d-value of each diffraction peak measured and the lattice parameters determined by d-value are listed in Table 1.

Fig.2 shows the X-ray diffraction spectra (from 24° to 36°) of the bulk specimen during heating at the heating rate of 5 ℃/min. In the spectra, the superstructure diffraction peaks of 111_M, 019_M (the next nearest neighbors ordering) and $10\bar{8}_M$ (the nearest neighbors ordering) appear. The d-value of each diffraction peak measured during heating is shown in Table 2. The integrated intensity of the superstructure diffraction peaks of 111_M and 019_M decreases during aging. Being heated to 160 ℃, $[(I_{111}+I_{019})_T-(I_{111}+I_{019})_{RT}]/(I_{111}+I_{019})_{RT}$ is 44%, $[(I_{01\bar{8}})_T-(I_{10\bar{8}})_{RT}]/(I_{10\bar{8}})_{RT}$ is 3.95%.

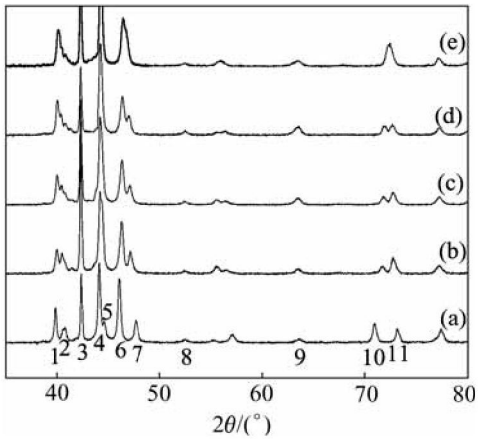

Fig.1 X-ray diffraction spectra of Cu-13Zn-15Al alloy during heating: (a) As-quenched; (b) Heated to 120 ℃; (c) Heated to 135 ℃; (d) Heated to 150 ℃; (e) Heated to 160 ℃ (In spectra the numbers 1 to 11 correspond to peak indexes of $12\bar{2}$, 202, 0018, $12\bar{8}$, 208, 1210, $20\bar{1}\,\bar{0}$, 1216 $(20\bar{1}\,\bar{6})$, $12\bar{2}\,\bar{0}$ (2020), 040 and 320 of M18R phase, respectively.)

Table 1 X-ray diffraction data of alloy during heating at heating rate of 5 ℃/min

hkl	*d*-value				
	RT	120 ℃	135 ℃	150 ℃	160 ℃
$12\bar{2}$	0.224	0.224	0.224	0.224	0.223
202	0.219	0.220	0.202	0.221	0.222
0018	0.211	0.211	0.211	0.212	0.212
$12\bar{8}$	0.203	0.203	0.203	0.203	0.203
208	0.201	0.202	0.203	0.203	0.203
1210	0.195	0.195	0.195	0.195	0.195
$20\bar{1}\,\bar{0}$	0.189	0.190	0.190	0.191	0.192
1216	0.166	0.166	0.167	0.168	0.170
2020	0.147	0.148	0.148	0.149	0.151
040	0.133	0.132	0.131	0.131	0.130
320	0.129	0.129	0.129	0.129	0.130
	a=0.443	a=0.444	a=0.444	a=0.445	a=0.446
	b=0.532	b=0.532	b=0.531	b=0.529	b=0.528
	c=3.800	c=3.804	c=3.805	c=3.811	c=3.814
	β^*=88.60°	β^*=88.65°	β^*=88.90°	β^*=89.27°	β^*=89.53°
	a/b=0.833	a/b=0.835	a/b=0.837	a/b=0.841	a/b=0.845

β^*: monoclinic angle

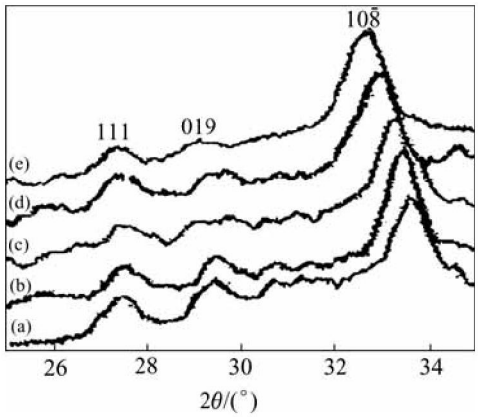

Fig.2 X-ray diffraction spectra of Cu-13Zn-15Al alloy during heating: (a) As-quenched; (b) Heated to 120 ℃; (c) Heated to 135 ℃; (d) Heated to 150 ℃; (e) Heated to 160 ℃

Table 2 Integrated intensity of superstructure diffraction peaks of alloy during heating at heating rate of 5 ℃/min

hkl	Integrated intensity				
	RT	120 ℃	135 ℃	150 ℃	160 ℃
111	8.22	7.83	6.81	6.64	5.43
019	7.12	6.20	5.96	4.87	3.14
10$\bar{8}$	35.89	35.97	36.11	36.68	37.31

4 Discussion

Fig.3 shows the hard sphere atomic structure model of the M18R martensite[17]. There are only 4 kinds of different positions, i.e. Ⅰ, Ⅱ$_1$, Ⅱ$_2$, Ⅲ, on the basal plane (Fig.3(b)). No matter how many sorts and how many amount of atoms are distributed, the structure factor can be expressed as

$$F_{hkl}=F_a\cdot F_l=\{f_{\square}+f_{\square}\exp 2\pi i(K/2)+f_{\square_1}\exp 2\pi i(H/2+K/4)+f_{\square_2}\exp 2\pi i(H/2+3K/4)\}\cdot\{1+\exp 2\pi i(H/x+K/2+L/18)+\exp 2\pi i(2H/x+2L/18)\}\cdot\{1+\exp 2\pi i(H/3+K/2+3L/18)+\exp 2\pi i(2H/3+6L/18)\}\cdot\{1+\exp 2\pi i(K/2+L/2)\} \quad (2)$$

where $x=a/x'$, $x'=c\cos(\beta/18)+a/3$[18].

With $K=2n$ and $H+K/2=2n+1$ (n: integer), the structure factor of the basal plane can be simplified into

$$F_a=(f_{\mathrm{I}}-f_{\mathrm{II}})+(f_{\mathrm{III}}-f_{\mathrm{II}}) \quad (3)$$

With $K=2n+1$, the structure factor of the basic plane can be simplified into

$$F_a=(f_{\mathrm{I}}-f_{\mathrm{III}}) \quad (4)$$

According to the experimental data of the lattice parameters, we obtain $1/2b>1/2\sqrt{a^2+(b/2)^2}$. This means the atoms between position Ⅰ and Ⅱ, and those between Ⅲ and Ⅱ are the nearest neighbors ordering state (nn), respectively; the atoms between position Ⅰ and Ⅲ are the next nearest neighbors ordering state when the martensite structure is ordering.

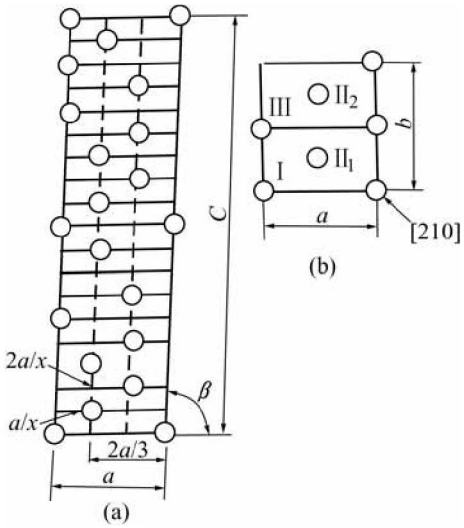

Fig.3 Crystal structure model of M18R martensite[17]: (a) Projection along [010] orientation; (b) Atoms arrangement on basal plane

According to the results of NAKATA et al[6], the atoms at position Ⅰ are (15/25)Al+(10/25)Cu, at position Ⅱ are Cu, and at position Ⅲ are (13/25)Zn+(12/25)Cu. If Cu atoms at position Ⅱ and Al atoms at Ⅰ interchange during heating, the relative integrated intensities of superstructure diffraction peaks of 111_M, 019_M and $10\bar{8}_M$ of different fraction of atoms are calculated by Eqn.(2) and listed in Table 3. The relative intensity of $10\bar{8}_M$ peak decreases if this exchange takes place, which contradicts to experimental results shown in Table 1. This exchange does not exist.

If Cu atoms at the position Ⅱ and Zn atoms at Ⅲ interchange during heating, the relative integrated intensities of superstructure diffraction peaks of 111_M, 019_M and $10\bar{8}_M$ of different fraction of atoms are calculated by Eqn.(2) and listed in Table 4. If 1.5/25 of Cu atoms transfer from position Ⅱ to Ⅲ, and 1.5/25 of Zn atoms transfer from position Ⅲ to Ⅱ, $[(I_{10\bar{8}}/I_{12\bar{8}})_{1.5}-(I_{10\bar{8}}/I_{12\bar{8}})_0]/(I_{10\bar{8}}/I_{12\bar{8}})_0$ is 3.6% from Table 4, where $(I_{10\bar{8}}/I_{12\bar{8}})_{1.5}$ expresses the relative integrated intensity of $10\bar{8}_M$ as 1.5/25 of Cu atoms transfer from position Ⅱ to Ⅲ, and 1.5/25 of Zn atoms transfer from position Ⅲ to Ⅱ; $(I_{10\bar{8}}/I_{12\bar{8}})_0$ expresses the relative integrated intensity of $10\bar{8}_M$ as the atoms do not change their position. Considering the experimental error, the calculated value coincides with the experimental results when heated to 160 ℃, but the decrease of the relative intensity of peaks of 111_M and 019_M is much less than that of the experiment.

It has been shown that the atoms between position

Ⅰ and Ⅲ are the next nearest neighbors ordering state when the martensite structure is ordering. When Al atoms at position Ⅰ and Zn at Ⅲ interchange during heating, the relative intensity of superstructure diffraction peaks of 111_M, 019_M and $10\bar{8}_M$ are calculated by Eqn.(2) and listed in Table 5. The decrease of relative integrated intensity of superstructure diffraction peaks of 111_M and 019_M is mostly caused by this exchange. The increase of relative integrated intensity of superstructure diffraction peaks of $10\bar{8}_M$ is only caused by the exchange of Cu atoms at the position Ⅱ and Zn at Ⅲ during heating (see Table 4 and Table 5).

Ignoring the effect of the exchange of Cu atoms at the position Ⅱ and Zn at Ⅲ on the decrease of relative integrated intensity of superstructure diffraction peaks of 111_M and 019_M, 13% (2/25) of Al atoms transfer from position Ⅰ to Ⅲ, $[(I_{111}/I_{12\bar{8}})_2+(I_{019}/I_{12\bar{8}})_2]-[(I_{111}/I_{12\bar{8}})_0+(I_{019}/I_{12\bar{8}})_0]/[(I_{111}+I_{12\bar{8}})_0+(I_{019}/I_{12\bar{8}})_0]$ is 46% from Table 5, which coincides with that of the experimental measurement heated to 160 ℃ (44%), where $(I_{111}/I_{12\bar{8}})_0$ and $(I_{019}/I_{12\bar{8}})_2$ express the relative integrated intensity of 111_M and 019_M, respectively, as 13% (2/25) of Al atoms transfer from position Ⅰ to Ⅲ; $(I_{111}/I_{12\bar{8}})_2$ and $(I_{019}/I_{12\bar{8}})_0$ express the relative integrated intensity of 111_M and 019_M, respectively, as the atoms do not change their position.

The integrated intensity of superstructure diffraction peaks of $10\bar{8}_M$ measured is more than that of the superstructure diffraction peaks of 111_M and 019_M, which is contrary to the calculated result. The reason is that the bulk specimen with preferable orientation is utilized to measure the relative variation of the integrated intensity of the superstructure diffraction in X-ray diffraction

Table 3 Relative integrated intensity of superstructure diffraction peaks of (111), (019) and $(10\bar{8})$ during exchange between Cu atoms at position Ⅱ and Al atoms at position Ⅰ

Relative intensity	Fraction of atoms		
	Ⅰ: 15/25Al+10/25Cu; Ⅱ$_1$: 25/25Cu; Ⅲ: 13/25Zn+12/25Cu	Ⅰ: 14.5/25Al+10.5/25Cu; Ⅱ$_1$: 0.5/25Al+24.5/25Cu; Ⅲ: 13/25Zn+12/25Cu	Ⅰ: 14/25Al+11/25Cu; Ⅱ$_1$: 1/25Al+24/25Cu; Ⅲ: 13/25Zn+12/25Cu
$I_{111}/I_{12\bar{8}}$	4.26	4.00	3.76
$I_{019}/I_{12\bar{8}}$	5.64	5.29	4.98
$I_{10\bar{8}}/I_{12\bar{8}}$	1.39	1.20	1.02

Table 4 Relative integrated intensity of superstructure diffraction peaks of (111), (019) and $(10\bar{8})$ during exchange between Cu atoms at position Ⅱ and Zn atoms at Ⅲ

Relative intensity	Fraction of atoms			
	Ⅰ: 15/25Al+10/25Cu; Ⅱ$_1$: 25/25Cu; Ⅲ: 13/25Zn+12/25Cu	Ⅰ: 15/25Al+10.5/25Cu; Ⅱ$_1$: 1/25Al+24//25Cu; Ⅲ: 12/25Zn+13/25Cu	Ⅰ: 15/25Al+11/25Cu; Ⅱ$_1$: 1.5/25Al+24/25Cu; Ⅲ: 11.5/25Zn+13/25Cu	Ⅰ: 15/25Al+10/25Cu; Ⅱ$_1$: 3/25Al+24/25Cu; Ⅲ: 10/25Zn+13/25Cu
$I_{111}/I_{12\bar{8}}$	4.26	4.22	4.20	4.14
$I_{019}/I_{12\bar{8}}$	5.64	5.58	5.56	5.47
$I_{10\bar{8}}/I_{12\bar{8}}$	1.39	1.41	1.44	1.48

Table 5 Rleative integrated intensity of superstructure diffraction peaks of (111), (019) and $(10\bar{8})$ during exchange between Zn atoms at position Ⅲ and Al atoms at Ⅰ

Relative intensity	Fraction of atoms		
	Ⅰ: 15/25Al+10/25Cu; Ⅱ$_1$: 25/25Cu; Ⅲ: 13/25Zn+12/25Cu	Ⅰ: 14.5/25Al+0.5/25Zn+10/25Cu; Ⅱ$_1$: Cu; Ⅲ: 11/25Zn+2/25Al+12/25Cu	Ⅰ: 12.5/25Al+2.5/25Zn+10/25Cu; Ⅱ$_1$: Cu; Ⅲ: 10.5/25Zn+2.5/25Al+12/25Cu
$I_{111}/I_{12\bar{8}}$	4.26	3.70	3.18
$I_{019}/I_{12\bar{8}}$	5.64	4.90	4.22
$I_{10\bar{8}}/I_{12\bar{8}}$	1.39	1.39	1.39
Relative intensity	Fraction of atoms		
	Ⅰ: 13.5/25Al+5/25Zn+10/25Cu; Ⅱ$_1$: Cu; Ⅲ: 11.5/25Zn+1.5/25Al+12/25Cu	Ⅰ: 13/25Al+2/25Zn+10/25Cu; Ⅱ$_1$: Cu; Ⅲ: 11/25Zn+2/25Al+12/25Cu	Ⅰ: 12.5/25Al+2.5/25Zn+10/25Cu; Ⅱ$_1$: Cu; Ⅲ: 10.5/25Zn+2.5/25Al+12/25Cu
$I_{111}/I_{12\bar{8}}$	2.71	2.28	1.87
$I_{019}/I_{12\bar{8}}$	3.59	3.03	2.48
$I_{10\bar{8}}/I_{12\bar{8}}$	1.39	1.39	1.39

experiment.

5 Conclusions

1) The parameters a and c of the martensite in Cu-13Zn-15Al alloy increase, the parameter b decreases, the monoclinic angle β approaches 90° when the Cu-13Zn-15Al alloy is heated at the heating rate of 5 ℃/min.

2) The bulk specimen with specific orientation is utilized to investigate the exchange of atoms in the martensite of Cu-13Zn-15Al alloy during non-isothermal aging. Besides the exchange of Zn atom at position Ⅲ and Cu at Ⅱ, the exchange between Zn atom at position Ⅲ and Al at Ⅰ on the basal plane of martensite occur during heating.

References

[1] SABURI T, WAYMAN C M. Shape memory mechanism in 18R martensitic alloys [J]. Acta Metall, 1980, 28(1): 15−32.

[2] OTSUKA K, REN X B. Recent developments in the research of shape memory alloys [J]. Intermetallics, 1999, 7: 511−528.

[3] VAN HUMBEECK J. Damping capacity of thermoelastic martensite in shape memory alloys [J]. J Alloys Comp, 2003, 355: 58−64.

[4] GONG C L, HAN F S, LI Z. Two internal-friction peaks related to thermoelastic martensitic transformations in CuAlNiMnTi shape-memory alloy [J]. Physical Review B, 2004, 70: 094103(1−6).

[5] ADIGUZEL O. Martensite ordering and stabilization in copper based shape memory alloys [J]. Materials Research Bulletin, 1995, 30(6): 755−760.

[6] NAKATA Y, YAMAMOTO O, SHIMIZU K. Effect of aging in CuZnAl shape memory alloys [J]. Materials Trans JIM, 1993, 5: 429−437.

[7] AHLERS M. Stability of martensite in noble metal alloys [J]. Mater Sci Eng A, 2003, 349: 120−131.

[8] ABU ARAB A, AHLERS M. Stabilization of martensite in CuZnAl alloys [J]. Acta Metall, 1988, 36: 2627−2638.

[9] AYDOGDU A, AYDOGDU Y, ADIGUZEL O. The influence of aging on martensite ordering and stabilization in shape memory Cu-Al-Ni alloys [J]. Materials Research Bulletin, 1997, 32(5): 507−513.

[10] STIPCICH M, ROMERO R. The effect of post-quench aging on stabilization of martensite in Cu-Zn-Al and Cu-Zn-Al-Ti-B shape memory alloys [J]. Mater Sci Eng A, 1999, 273−275: 581−585.

[11] OTSUKA K, REN X. Mechanism of martensite aging effect [J]. Scripta Mater, 2004, 50: 207−212.

[12] PELEGRINA J L, AHLERS M. Stabilization and ferroelasticity in Cu-Zn based martensites [J]. Scripta Mater, 2004, 50: 213−218.

[13] LI Z, WANG M P. Effect of cooling rate on the order in martensite of a CuZnAl alloy [J]. Journal of Material Science, 2005, 40: 123−127.

[14] KUSTOV S, PONS J, CESARI E. Pinning-induced stabilization of martensite: Part Ⅱ. Kinetic stabilization in CuZnAl alloy due to pinning of moving interfaces [J]. Acta Mater, 2004, 52: 3083−3096.

[15] TADAKI T, OKAZAKI H, NAKATA Y. Atomic configuration studied ALCHEMI and X-ray diffraction of a stabilization M18R martensite in a β phase CuAuZn alloy [J]. Materials Trans JIM, 1990, 31: 941−947.

[16] WANG R H, GUI J N, CHEN X M. EBSD and TEM study of self-accommodating martensites in $Cu_{75.7}Al_{15.4}Mn_{8.9}$ shape memory alloy [J]. Acta Mater, 2002, 50: 1835−1847.

[17] KUBO H, SHIMIZU K. Crystal structure of $Cu_{30}Au_{25}Zn_{45}$ martensite [J]. Trans JIM, 1976, 17: 330−338.

[18] TADAKI T, TAKORO M, SHIMIZU K. Thermoelastic nature and crystal structure of CuZn martensite related to the shape memory [J]. Trans JIM, 1975, 15: 285−296.

(Edited by YUAN Sai-qian)